Characterization of calcium- and integrin-binding protein 1 (CIB1) knockout platelets: Potential compensation by CIB family members

Jan C. DeNofrio[*,1], **Weiping Yuan**[*,2], **Brenda R. Temple**[2], **Holly R. Gentry**[2], and **Leslie V. Parise**[2,3,4,5,‡]

[1]Curriculum in Genetics and Molecular Biology, The University of North Carolina, Chapel Hill, North Carolina, USA

[2]Department of Biochemistry and Biophysics, The University of North Carolina, Chapel Hill, North Carolina, USA

[3]Department of Pharmacology, The University of North Carolina, Chapel Hill, North Carolina, USA

[4]Lineberger Comprehensive Cancer Center, The University of North Carolina, Chapel Hill, North Carolina, USA

[5]Carolina Cardiovascular Biology Center, The University of North Carolina, Chapel Hill, North Carolina, USA

Summary

Platelet aggregation requires activation of the αIIbβ3 integrin, an event regulated by the integrin cytoplasmic tails. CIB1 binds to the cytoplasmic tail of the integrin αIIb subunit. Previous overexpression and knockdown studies in murine megakaryocytes demonstrated that CIB1 inhibits integrin αIIbβ3 activation. Here we analyzed *Cib1*$^{-/-}$ mice to determine the function of CIB1 in platelets *in vitro* and *in vivo*. We found that although these mice had no overt platelet phenotype, mRNA level of CIB1 homolog CIB3 was increased in *Cib1*$^{-/-}$ megakaryocytes. *In vitro* binding experiments showed that recombinant CIB1, -2 and -3 bound specifically to an αIIb cytoplasmic tail peptide. Subsequent protein modeling experiments indicated that CIBs 1–3 each have a highly conserved hydrophobic binding pocket. Therefore, the potential exists for compensation for the loss of CIB1 by these CIB family members, thereby preventing pathologic thrombus formation in *Cib1*$^{-/-}$ mice.

Keywords

CIB1; platelet; integrin αIIbβ3 activation; aggregation; knockout mouse; compensation

Introduction

Platelets respond to blood vessel injury to prevent further blood loss and restore vascular integrity. They become activated at the site of vascular injury by newly exposed extracellular matrix proteins (ECM) and secreted soluble agonists. Platelet activation promotes binding of soluble and matrix adhesive proteins to activated surface receptors. The interaction of platelets

Address correspondence to: Leslie V. Parise, Dept. of Biochemistry and Biophysics, CB# 7260, The University of North Carolina, Chapel Hill, NC, 27599. Tel.: 919-966-2238; Fax: 919-966-2852; Email: parise@med.unc.edu.
[*]Both authors contributed equally to this work.

with soluble proteins such as fibrinogen initiates platelet aggregation, whereas platelet interaction with ECM proteins such as collagen allows both platelet adhesion and thrombus generation.

Integrins are heterodimeric adhesion receptors that undergo conformational changes upon agonist stimulation, resulting in increased ligand affinity. This process is termed inside-out signaling (1). The most abundant integrin on the platelet surface is αIIbβ3. Active integrin αIIbβ3 initiates and propagates the formation of platelet aggregates by binding to fibrinogen. Although fibrinogen is the primary ligand for αIIbβ3, the activated integrin also binds other extracellular proteins such as fibronectin, von Willebrand factor and vitronectin to support platelet adhesion to the blood vessel wall (2;3). Since uncontrolled activation of integrin αIIbβ3 can cause pathologic thrombus formation, precise regulation of the integrin is critical for haemostasis (4).

CIB1 (CIB, calmyrin, and KIP1) was identified in a yeast-two hybrid screen to identify binding partners for the integrin αIIb cytoplasmic tail (5). CIB1 is a widely expressed protein that contains two calcium binding and two non-calcium binding EF hands (6;7). CIB1 interacts with a number of serine/threonine kinases such as DNA-dependent protein kinase (8), polo-like kinases Fnk and Snk (9), and PAK1 (10), as well as presenilin 2 (11), FAK(12) and the InsP3 receptor (13). Recent *in vivo* studies demonstrate that CIB1 also plays a role in pathological forms of angiogenesis (14) and is essential for spermatogenesis (15).

Previously, the function of CIB1 relative to αIIbβ3 was explored by acutely overexpressing and knocking down the protein in murine megakaryocytes. These studies implicated CIB1 as a negative regulator of agonist-induced αIIbβ3 activation (16). In separate studies where CIB1 function was also rapidly blocked by use of a CIB1 antibody, it was found that CIB1 binding to αIIbβ3 is necessary for proper spreading on immobilized fibrinogen (17). Taken together these studies imply that acute alterations in CIB1 protein misregulate αIIbβ3 function.

To more fully characterize the role of CIB1 in platelets, we asked if the chronic loss of CIB1, via a CIB1 knockout mouse, would result the same phenotype as acutely altered CIB1. While we hypothesized that loss of CIB1 would result in increased agonist-induced activation of integrin αIIbβ3 and hyper-activatable platelets, the $Cib1^{-/-}$ mice did not display any overt defect in platelet function. These results suggest that either CIB1 does not regulate the platelet functions tested or that developmental compensation has occurred. In this regard, mRNA expression for the CIB1 homolog CIB3 is increased in cultured megakaryocytes isolated from the $Cib1^{-/-}$ mice. This protein may have a redundant or overlapping function in αIIbβ3 regulation and may compensate for the lack of CIB1. To test this, we produced recombinant CIB1, -2 and -3 and compared their ability to bind to the αIIb cytoplasmic tail.

Materials and methods

Mice

$Cib1^{-/-}$ mice were previously generated in our lab as described by Yuan et al. (15). All mouse experiments were performed in accordance with national guidelines and regulations and were approved by the UNC Institutional Animal Care and Use Committee (IACUC). Mice used in these experiments were backcrossed 10 generations to the C57BL/6 background.

Platelet isolation

Mice were euthanized by CO_2. Blood was drawn by cardiac puncture into Eppendorf tubes containing saline and ACD (85 mM sodium citrate, 111 mM glucose and 71 mM citric acid) with 0.1 μM PGE_1 (Sigma). To separate blood cells, whole blood was centrifuged for 10 min at $250 \times g$. Platelet rich plasma (PRP) was removed and the remaining blood was washed with

ACD/saline/PGE$_1$ solution, centrifuged and PRP collected. PRP was pooled for each mouse and centrifuged at $400 \times g$ for 15 min. Platelet poor plasma (PPP) was discarded, and the platelet pellet resuspended in warmed (37°C) CGS buffer (13 mM sodium citrate, 30 mM glucose and 120 mM NaCl) containing 10 U/ml apyrase (Sigma). Resuspended platelets were incubated at 37°C for 20 min before being centrifuged at $500 \times g$ for 15 min. The platelet pellet was resuspended in 0.5 ml modified HEPES-Tyrodes buffer (12 mM NaHCO$_3$, 138 mM NaCl, 5.5 mM glucose, 2.9 mM KCl, 10mM HEPES containing 0.1% BSA, 1mM CaCl$_2$, 1mM MgCl$_2$ at pH 7.4). Platelets were allowed to rest for 1 h at room temperature (RT) before assaying.

Electron Microscopy

PRP was isolated as above and centrifuged at $400 \times g$ for 15 min. PPP was removed and the platelet pellet was fixed by the addition of 2% glutaraldehyde in 0.1 M sodium cacodylate buffer pH 7.4 (all buffers provided by UNC Microscopy Services Laboratory). After 2 h at RT, the glutaraldehyde solution was removed, the pellet washed with cacodylate buffer and fixed in potassium ferrocyanide-reduced osmium tetroxide for 1 h at RT. The pellet was dried with ethanol and embedded in PolyBed 812 epoxy resin (Polysciences, Inc., Warrington, PA, USA). Sections of the pellet (70 nm thick) were mounted on copper grids and stained with 4.0% uranyl acetate and 0.4% lead citrate. Sections were observed with a LEO EM 910 transmission electron microscope (LEO Electron Microscopy, Inc., New York, NY, USA) using an accelerating voltage of 80 kV. Platelet granules were scored for two mice of each genotype, and a minimum of 45 platelets were counted per genotype.

Platelet spreading

Glass coverslips were coated with 1% BSA (Serologicals Protein Inc.) or 100 µg/ml fibrinogen (Calbiochem). Platelets were isolated and washed as above and resuspended in Tyrodes-HEPES buffer to 1×10^7 plts/ml. Precoated coverslips were washed twice with Tyrodes-HEPES buffer and 100 µl platelets were added and incubated for 1 h at 37°C. Coverslips were aspirated to remove unattached cells and remaining cells were fixed with 1.0% paraformaldehyde for 15 min at RT. Coverslips were washed twice and permeablized with 0.2% Triton-PBS for 30 seconds and washed three times with Tyrodes-HEPES. For staining, coverslips were incubated in the dark with 1:1,000 phallodin-488 (Molecular Probes) for 30 min. Coverslips were rinsed and adhered to slides with FlouroSave (Calbiochem).

Flow cytometry

Washed platelets were incubated with a FITC-labeled antibody for 15 min (JON/A, glycoprotein (GP) 1b and respective IgG controls, EMFRET, Germany) or 30 min (αIIb or α2 and respective IgG controls, BD BIOSCIENCE) at RT. For αIIbβ3 activation experiments, agonist (0.1 U thrombin or 10 µM ADP final concentrations) was added simultaneously with the antibody. P-selectin expressed on the platelet surface was measured in whole blood using a FITC-labeled P-selectin antibody (EMFRET, Germany). Whole blood samples were prepared as described by manufacturer's instructions. P-selectin expression was induced by activation 0.25 mM PAR4 peptide (thrombin receptor activating peptide, AYPGKF, synthesized by the UNC Protein Chemistry Core) or 100 µM ADP, as a negative control, as determined by the manufacturer's protocol (EMFRET). After incubating, all samples were diluted with Tyrodes-HEPES and analyzed on a BD FACSCanto flow cytometer (BD Biosciences) at a low flow rate. Surface expression data were normalized by dividing the mean fluorescent intensity of the antibody by the control IgG intensity. Activation data were normalized by dividing the agonist stimulated mean fluorescence by that of the unstimulated cells.

Aggregation

Platelets were isolated as above and diluted into Tyrodes-HEPES buffer to 1.5×10^8 plts/ml. Platelets were aliquoted into aggregation tubes and incubated at 37° C for 15 min before the addition of agonist, 0.1 mM PAR4 peptide (AYPGKF, synthesized at UNC Protein Chemistry Core) or 5 µM ADP. Traces were recorded for 5–6 min in a CHRONO-LOG Corporation Model 700 Aggregometer. Aggregometry data were analyzed by Aggrolink8 software (CHRONO-LOG).

Bleeding times assay

Mice were anesthetized with isoflurane and given an intraperitoneal injection of 10 µl/g mouse of ketamine hydrochloride (75µg/kg). Mouse tails were cut at 4mm from the tip and placed into Phosphate-buffered saline (PBS) warmed to 37°C. Time was recorded until the stream of blood fully stopped. Mouse tails were cauterized after 15 min if bleeding did not stop.

Carotid artery thrombosis

Adult mice (24–34 g) were anesthetized with isoflurane and maintained under inhaled anesthesia at a temperature of 36–37.5°C. The carotid artery was exposed and rinsed with saline. To measure baseline flow rate, a Doppler flow probe (#0.5VB307, Transonic Systems Inc) connected to a flow meter (T106, Transonic Systems Inc) was placed on the blood vessel and both were covered with a lubricating jelly. After baseline was determined, the artery was rinsed with saline and a 1×2 mm piece of Whatmann paper saturated with 20% ferric chloride was placed on the vessel for 2 minutes. After 2 min the filter paper was removed from the artery and replaced with lubricating jelly. Blood flow was measured until the vessel occluded.

Western blot analysis

Washed platelets were lysed in modified CHAPS buffer (20 mM HEPES, pH 7.4, 150 mM NaCl , 10 mM CHAPS , 50 mM NaF , 10 mM β-glycerophosphate, 1:100 concentration Protease Inhibitors Cocktail Set III (Calbiochem), 1 mM $CaCl_2$ and 1 mM $MgCl_2$) on ice for 30 min. Lysates were collected after a 10 min centrifugation and the protein concentration was quantified by the BCA protein assay (Pierce). Protein samples were separated by SDS-PAGE, transferred to a PVDF membrane and subjected to Western blotting. A CIB1 chicken polyclonal antibody was used to detect mouse CIB1. The antibody against GAPDH was from Santa Cruz Biotechnology.

Primary megakaryocyte culture

Murine bone marrow-derived megakaryocytes were cultured as previously described (18). Briefly, bone marrow cells were flushed and isolated from tibias and femurs of mice and cultured for three days in medium containing Interleukin (IL)-6, IL-11 and thrombopoietin (PeproTech).

Quantitative reverse transcriptase-PCR

Megakaryocytes derived from bone marrow stem cells were isolated as above. RNA was isolated with the Qiagen RNA Isolation kit. Isolated RNA was transcribed into cDNA using Applied Biosystems' High-Capacity Reverse Transcription Kit. Primers for *Cib1, Cib2, Cib3, Cib4* and *Gapdh* were purchased from SuperArray. Sequences were proprietary, reference positions for partial product sequence amplified by primers, relative to NCBI RefSeq entry provided by SuperArray; Cib1 260–278 (RefSeq Accession# NM_011870), Cib2 590–609 (RefSeq Accession# NM_019686), Cib3 326–344 (RefSeq Accession# XM_356089.4), Cib4 271–291 (RefSeq Accession# XM_131990.3) and Gapdh 962–983 (RefSeq Accession# NM_008084.2). SYBR Green PCR Mastermix was also from SuperArray and manufacturer's

protocol was followed. Real time qPCR reactions were run on Applied Biosystems Instruments Prism 7900HT Sequence Detection System using the standard 1 cycle at 95° C for 10 min and 40 cycles of 95° C for 15 s then 60° C for 1 min. Fold change in gene expression was calculated using the ΔΔCt method(19;20).

Protein purification

PCR primers were designed to amplify *Cib1-3* mRNAs isolated from murine megakaryocytes. PCR products of *Cib1*, *-2* and *-3* were ligated into the pEXP5-NT/TOPO vector (Invitrogen) and correct sequences were verified. BL21 bacteria (Stratagene) were transformed with pEXP5-NT/TOPO vectors, grown at 37°C and induced with isopropyl β-D-1-thiogalactopyranoside (IPTG) for 4 h at 30°C to produce the desired proteins. pEXT5-NT/ TOPO calmodulin-like 3 from Invitrogen was used as a control. Bacteria producing CIB1, CIB2 and calmodulin-like 3 were lysed by sonication and centrifuged at $10,000 \times g$ for 20 min. Supernatant was run on an FPLC-nickel column to purify the protein. Since CIB3 was insoluble, the bacteria producing CIB3 were lysed and denatured in buffer containing 8 M urea (Sigma), 100 mM NaH_2PO_4 (Mallinckrodt) and 10 mM Tris-Cl (Fisher) at pH of 8.0. Lysate was centrifuged to remove cellular debris and Ni-NTA slurry (Qiagen) was added to the supernatant and incubated at RT for 1 h with shaking. The lysate-resin mixture was loaded onto a column and flow-through was removed. The column was washed twice with buffer containing 8 M urea, 100 mM NaH_2PO_4 and 10 mM Tris-Cl at pH 6.3. Protein was eluted with buffer containing 8 M urea, 100 mM NaH_2PO_4 and 10 mM Tris-Cl at pH 5.9. Eluate was dialyzed into 8 M urea, 200 mM NaCl and 50mM Tris pH 8.0 at 4° C. After 4 h, an equal volume of buffer containing 200 mM NaCl and 50 mM Tris pH 8.0 with 2 mM dithiothreitol (DTT, ROCHE) was added to dilute the urea and left to dialyze overnight. Buffer was then exchanged with 2 M urea, 200 mM NaCl, 50 mM Tris pH 8.0 and 2 mM DTT to continue dialyzing and allow protein refolding. This process continued every 8 h until the urea was fully removed. The DTT was dialyzed out of solution by 200 mM NaCl, 50 mM Tris pH 7.5. The protein was dialyzed into a final buffer containing 20 mM Tris pH 7.5, 300 µM $CaCl_2$ and 85 mm NaCl.

ELISA

An αIIb cytoplasmic tail (CT) peptide (sequence LVLAMWKAGFFKRNR synthesized by Genscript Corporation) or a scrambled control peptide (sequence DKFGRPPKVENEELEDRGEF, synthesized by UNC Protein Chemistry Core Facility) was coated on a microtiter plate (NUNC) overnight at 4°C at a concentration of 75 µg/ml. BSA (3%) was used to block non-specific interactions in peptide-coated and non-coated wells. Proteins were diluted in 50 mM HEPES, 150 mM NaCl with 0.1 mM $CaCl_2$ and $MgCl_2$ pH 7.4 to a range of 0.5 µg/ml to 20 µg/ml and were allowed to adhere to the plate for 1 h at RT. The samples were removed, and the plate was washed three times with 0.5% TBS-Tween, pH 7.4. A primary anti-HIS antibody was added and incubated for 1 h at RT. The antibody was removed and the plate was washed as above. An anti-rabbit-HRP antibody was then added to the microtiter place for 1 h at RT. The secondary antibody was removed, and the plate was washed as above. Binding was visualized by a color reaction with chromogenic substrate OPD Sigma Fast Tablets (Sigma) for 10 min at RT in the dark. The reaction was stopped with 4N H_2SO_4 and the plate was read at 490 nm in Medical Devices SpectraMax Plus plate reader. For competition binding assays, 5 µg/ml of CIB1, -2 and -3 were incubated with increasing concentrations (1.0–100 µg/ml) of soluble αIIb peptide. Each sample and concentration was performed in triplicate for all ELISAs.

CIB homology and model analysis

CIB homologs in the UniProt database (21) were identified using sequence similarity BLAST searches (22) of the human CIB1 protein. We used ClustalX (23) to generate a multiple sequence alignment of the three human CIB homologs (CIB1 (Q99828), CIB2 (O75838), CIB3 (Q96Q77)), and homologs of the fruitfly and worm CIB gene (*D. melanogaster* (Q9W2Q5), *D. pseudoobscura* (Q28ZR4), *C. elegans* (Q93640)). We then mapped highly conserved residue positions onto the crystallographic structure of human CIB1 (PDB ID 1XO5 (6)).

Statistical analysis

All values are presented as the mean ± standard error of the mean (SEM). A *t*-test was used to evaluate statistical significance. P-values less than 0.05 were considered statistically significant. N ≥ 3 for all experiments.

Results

Platelet function is normal in *Cib1⁻/⁻* mice

We first confirmed that CIB1 was absent in the *Cib1⁻/⁻* platelets by Western blotting (Fig. 1A). The overall morphology of the platelets by transmission electron microscopy appeared normal; platelet shape and organelles were similar in both genotypes (Fig. 1B, C). The number of α- and dense granules per platelet were scored. There was no statistical difference in the number of either dense or α-granules in the *Cib1⁻/⁻* versus control platelets (Fig 1C). Flow cytometry with antibodies specific to integrins αIIbβ3 and α2β1, and glycoprotein (GP) Ib indicated that there were no statistically significant differences detected in the expression levels of these receptors on platelets isolated from the *Cib1⁺/⁺* and *Cib1⁻/⁻* mice (Fig. 1D). These results thereby assure that any difference displayed in our αIIbβ3 functional studies was not due to a change in surface expression of αIIbβ3.

To examine potential differences in αIIbβ3 activation between *Cib1⁺/⁺* and *Cib1⁻/⁻* mice, we measured binding of an activation-specific antibody binding (JON/A) to αIIbβ3 in resting or agonist stimulated platelets by flow cytometry. Basal αIIbβ3 activity in resting platelets was comparable in *Cib1⁻/⁻* and *Cib1⁺/⁺* mice (measured by the binding of unstimulated cells to the JON/A antibody). We also found no significant difference in the ability of *Cib1⁻/⁻* platelets to bind JON/A in response to a relatively weak agonist (10 µM ADP), or strong agonist (0. 1 U thrombin) versus platelets isolated from *Cib1⁺/⁺* littermate controls (Fig. 2A). We then used platelet aggregation to evaluate αIIbβ3 activation. We found that *Cib1⁻/⁻* platelets aggregate in a similar manner as *Cib1⁺/⁺* platelets when stimulated by agonist 0.1 mM PAR4 peptide or 5 µM ADP (Fig. 2B). (As we did not add exogenous fibrinogen to our aggregation experiments, 5 µM ADP was the lowest concentration of agonist that could provide a consistent aggregation response).

Platelet activation leads to exposure of P-selectin on the platelet surface; therefore we used flow cytometry to examine any potential changes in P-selectin exposure. We found similar surface expression levels of P-selectin on resting platelets from *Cib1⁺/⁺* mice and *Cib1⁻/⁻* mice, and on platelets activated by 100 µM ADP or 0.25 mM PAR4 (Fig. 2C). P-selectin surface expression and agonist-induced α-granule release did not appear to be affected by the loss of CIB1. These results imply that the absence of CIB1 does not alter integrin αIIbβ3 expression or activation.

Acute blockade of CIB1 in platelets inhibits platelet spreading on immobilized fibrinogen (12;17). We therefore tested platelets from the *Cib1⁻/⁻* mice to determine the effect of the loss of CIB1 on platelet spreading, but found no difference between size and overall cell number of platelets adhered to fibrinogen in the presence or absence of ADP (Fig. 3A–C). Platelet

spreading was also similar between the two genotypes after PAR4 stimulation, or on collagen in the absence or presence of ADP (data not shown). Therefore, outside-in signaling as measured by platelet spreading appears to be normal in the $Cib1^{-/-}$ deficient mice.

In vivo experiments

We then used whole animal models to determine the response of $Cib1^{-/-}$ mice to blood vessel injury. A bleeding time assay measures the time necessary for bleeding to stop after the removal of a small portion of the mouse's tail (24). We found no statistically significant difference in the average bleeding time for $Cib1^{-/-}$ versus $Cib1^{+/+}$ mice (Fig. 4A). The ferric chloride injury model is frequently used for assessing *in vivo* responses to injury to the blood vessel endothelium (25). Ferric chloride causes tissue damage by iron-mediated chemical oxidation, resulting in separation of endothelial cell junctions and exposure of type I collagen (26;27). To determine the role of CIB1 in thrombus formation upon vascular injury, ferric chloride was placed on the carotid artery to expose the underlying ECM (27). Time to full vessel occlusion by a stable thrombus was similar between the $Cib1^{+/+}$ and $Cib1^{-/-}$ mice (Fig. 4B). Thus, $Cib1^{-/-}$ mice exhibit no discernible differences in thrombus formation or stability leading to vessel occlusion and blood clotting *in vivo* as measured by these assays.

CIB family gene *Cib3* is over-expressed in *Cib1⁻/⁻* primary megakaryocytes

Our previous studies involving the acute modulation of CIB1 levels in megakaryocytes showed that CIB1 is an endogenous inhibitor of αIIbβ3 activation (16). Here we tested αIIbβ3 activation in megakaryocytes from $Cib1^{-/-}$ mice to determine whether chronic loss of CIB1 has a similar phenotype to the acute megakaryocyte studies (16). However, we found that megakaryocytes differentiated in culture from the bone marrow stem cells of $Cib1^{-/-}$ mice bound fibrinogen in a similar manner as those from $Cib1^{+/+}$ mice. Specifically, both genotypes had similar levels of fibrinogen binding under basal conditions and upon stimulation with agonist PAR4 (Fig. 5A). This result models our $Cib1^{-/-}$ and $Cib1^{+/+}$ platelet data, and are in contrast to results obtained with short term, direct protein or genetic manipulations (12;16;17;28).

Since we did not see a change in αIIbβ3 activation in $Cib1^{-/-}$ mouse platelets or megakaryocytes, we considered the possibility of functional compensation by other CIB family members, as the chronic loss of CIB1 could alter the expression of other genes. Genes of human homologs $Cib2$, $Cib3$ and $Cib4$ have been reported (6) and genes of mouse $Cib2$–4 can be identified in the mouse gene database. The identified and predicted CIB protein transcripts are highly homologous between human and mouse. CIB1 is 94% identical while CIB2, CIB3 and CIB4 are 97%, 94% and 91% identical, respectively, as determined by BLAST analysis. Therefore, we examined the expression of these mouse genes using real-time qPCR with mRNA derived from cultured murine megakaryocytes. We found increased $Cib3$ mRNA expression in the $Cib1^{-/-}$ bone marrow-derived megakaryocytes while $Cib2$ message levels remained constant between $Cib1^{+/+}$ and $Cib1^{-/-}$ megakaryocytes (Fig. 4B). Endothelial cell function is affected by the loss of CIB1(14); therefore we examined the relative mRNA expression levels of $Cib2$ and $Cib3$ in $Cib1^{-/-}$ endothelial cells to that in $Cib1^{+/+}$ endothelial cells. Unlike megakaryocytes, $Cib2$ and $Cib3$ mRNA expression is not elevated in $Cib1^{-/-}$ endothelial cells compared to $Cib1^{+/+}$ cells (Fig. 5B). $Cib4$ was excluded from further studies because only a very low level of $Cib4$ message (slightly above background) was detected in both megakaryocytes and endothelial cells by reverse transcriptase-PCR and by qPCR in either genotype (data not shown).

Since mRNA from the $Cib1^{-/-}$ megakaryocytes displayed a different expression pattern for $Cib3$ relative to $Cib1^{+/+}$ megakaryocytes, we further investigated the possibility of functional compensation. We produced and purified recombinant CIB1, -2 and -3 proteins from bacterial cultures to test the binding properties of CIB family proteins with integrin αIIb. It is currently

unknown whether CIB2 or CIB3 is expressed in platelets. CIB2 protein expression has been identified in HEK cells (29) but CIB3 protein remains to be examined or reported. Antibodies that recognize mouse CIB2, -3, or -4 are not currently available. Nonetheless, we asked if recombinant murine CIB2 and CIB3 could bind to αIIb. We immobilized an αIIb-cytoplasmic tail (CT) peptide in microtiter wells, added increasing concentrations of recombinant CIB1, -2, and -3 proteins and measured binding by ELISA (Fig. 6A). Interestingly, all three CIB proteins bound to immobilized αIIb-CT peptide. However, none of the proteins bound to a scrambled control peptide, thereby implicating a specific interaction between these CIB proteins and αIIb (Fig. 6A). To further ensure the specificity of binding to the αIIb-CT peptide, we added increasing concentrations of soluble αIIb peptide to compete with CIB protein binding to immobilized peptide. Addition of this soluble peptide decreased the binding of CIB1, -2 or -3 to immobilized peptide (Fig. 6B), reaffirming a specific interaction between the αIIb-CT peptide and CIB proteins, whereas the soluble scrambled peptide did not interfere with CIB protein binding (data not shown). These findings demonstrate that CIB2 and CIB3 can bind to the cytoplasmic tail of αIIb *in vitro* and therefore have the potential to compensate for the loss of CIB1.

Computer modeling of the CIB family

For insight into the potential mechanism of how CIB2 and/or CIB3 might compensate for the loss of CIB1 in αIIbβ3 regulation, we performed computer modeling studies. We evaluated CIB family homology by aligning the ancestral CIB protein from worm (*Caenorhabditis elegans*) and fruit fly (*Drosophila melanogaster*) with the human CIB1-3 proteins. Highly conserved residues are represented in purple and yellow while non-conserved residues are represented in grey and orange (Fig. 7). The conservation is indicative of potential functionality that existed in the CIB ancestor and that has been maintained in the CIB1-3 homologs (purple and yellow residues Fig. 7).

Residues in CIB1 that are proposed to interact with αIIb based on previous studies and on the crystal structure of CIB1 (5–7,30–32) were specifically compared to the corresponding residues in CIB2 and CIB3. CIB residues hypothesized to form a hydrophobic binding pocket for the αIIb tail are designated by yellow for conserved and orange for non-conserved residues (Fig. 7A). Almost all of the residues in the hydrophobic binding pocket are highly conserved between the three human CIB homologs and the worm and fruit fly CIB homolog, indicating a potentially shared functional domain.

The C-terminus of CIB1 has been proposed to be displaced upon αIIb binding (32); therefore, we also performed a modeling analysis with the C-terminus of CIB2 and CIB3 removed (Fig. 7B). The additional residues exposed in CIB2 and CIB3 were highly homologous to those exposed in CIB1 upon C-terminal deletion (Fig. 7B). In addition, the length and depth of the hydrophobic binding pocket was enlarged similarly between each CIB protein. This suggests that all three CIB proteins may use the C-terminus to control binding specificity as proposed by Yamniuk et al. 2006 (32) for CIB1.

Discussion

Activation and regulation of platelet integrin αIIbβ3 has been extensively studied, and much is now known about how the integrin becomes activated (33–35); yet, the precise mechanisms controlling activation and deactivation of the integrin and molecules involved are still under investigation. Several intracellular binding partners of the integrin are known to regulate αIIbβ3 activation (36). Interestingly, most of these regulatory proteins bind to the β3 cytoplasmic tail and not to αIIb (36). The αIIb subunit currently has only a handful of binding partners, and there has been conflicting reports on the function of these proteins in αIIbβ3 activation (37–41). Previously we identified CIB1 in a screen for binding partners, and potential

regulators of the αIIb cytoplasmic tail. Initial genetic studies of CIB1 function required a megakaryocyte model because only platelets and megakaryocytes express the required signaling machinery involved in integrin αIIbβ3 inside-out activation and platelets are not amenable to direct genetic manipulation (42). For a more comprehensive understanding of the role of CIB1 in the regulation of integrin αIIbβ3 activation, we created a $Cib1^{-/-}$ mouse and studied the function of platelets and megakaryocytes derived from these mice. We found no significant difference in the protein expression, basal activation or agonist-induced activation of αIIbβ3, as measured by flow cytometry. There was also no significant difference in aggregation or spreading between platelets from $Cib1^{+/+}$ or $Cib1^{-/-}$ mice.

The lack of a phenotype in αIIbβ3 activation in $Cib1^{-/-}$ mice was unexpected because our megakaryocyte studies and other independent studies in platelets (7;12;16;17;28;43) demonstrated that CIB1 regulates αIIbβ3 activation and platelet spreading. One possible explanation for the apparent lack of phenotype in the $Cib1^{-/-}$ platelets could be due to a compensatory mechanism that occurred during mouse development. The most obvious possibility would be compensation by another CIB family member. The idea of functional compensation resulting in a limited phenotype is not novel. For example, Vav1 and Vav3 are functionally redundant in their role of activating PLCγ2 (44) in platelets. Other proteins, when knocked down or knocked out, also have not displayed the platelet phenotype predicted by previous short term genetic manipulations (44–47). The discrepancies in our previous megakaryocyte results and *in vivo* results may reflect fundamental differences in chronic genetic mutations (knock-out or knock-in), which are subject to developmental compensation compared to acute genetic mutations (knock-down or overexpression), which can reflect the function of a protein in the absence of compensation. Both short and long term genetic manipulations provide valuable information but the results should be only interpreted under each experimental condition.

In real-time PCR experiments we detected an increase in the message of *Cib3* while the message of *Cib2* did not change between $Cib1^{+/+}$ and $Cib1^{-/-}$ in megakaryocytes. Therefore, the potential binding of CIB2 and CIB3 to the αIIb tail was investigated. ELISA data indicated that CIBs1-3 can all bind to the cytoplasmic tail of αIIb. The apparent CIB2/αIIb interaction was unexpected since CIB2 did not bind αIIb in a yeast two-hybrid assay (16).

Sequence homology shows that human CIB2, CIB3 and CIB4 are 59%, 62% and 64%, homologous to CIB1, respectively (6). Human CIBs show equivalent residues involved in the structure of the hydrophobic binding pocket, i.e. the canonical αIIb binding site by sequence alignment (6). Currently, only human CIB2 has been reported as a protein in the literature (29); endogenous human or murine CIB3 and CIB4 proteins have not been identified to date. The computer homology modeling analyses of CIB proteins provide insights into potentially conserved αIIb binding domains in CIB1-3 that support our protein binding data. We observed a highly conserved hydrophobic binding pocket in all CIB1-3 proteins. CIB1 is reported to undergo displacement of its C-terminus upon αIIb binding, which increases the size of the hydrophobic binding pocket (32). Virtual removal of the corresponding C-terminal residues in CIB2 and CIB3 also led to an increase in the size of the hydrophobic binding pocket as revealed by our modeling studies. The residues exposed by displacement of the tail were also highly conserved between CIB1, -2 and -3. This theoretical structural change could potentially allow CIB2 and CIB3 to share binding partners with CIB1, e.g. integrin αIIbβ3. Future studies of the biophysical properties of the CIB family with isothermal titration calorimetry or other approaches will further our understanding of the properties with which this family interacts with αIIbβ3.

It will be interesting to determine if any other tissues or cell types in the $Cib1^{-/-}$ mice have altered CIB family protein expression. It is known that the chronic loss of CIB1 affects

spermatogenesis (15) and angiogenesis (14) in the *Cib1*$^{-/-}$ mice. This begs the question of why some cell types or processes may have developed compensatory mechanisms, while other cells have not. For example, endothelial cells isolated from the *Cib1*$^{-/-}$ mice do not have fully functional compensatory mechanisms, as they have decreased migration in culture and *in vivo* these mice have a defective pathological angiogenic response to ischemia (14). Also of interest is the question of how many binding partners are shared by CIB1, -2 and -3? Since the functional role of the CIB family *in vivo* has not been established, the development of investigational tools such as expression plasmids and antibodies to other CIB family proteins will aid the investigation of CIB protein function and regulation. RNAi will also be important in acute knockdown studies to evaluate the activation potential of αIIbβ3 in megakaryocytes from the *Cib1*$^{-/-}$ mouse with CIB3 acutely knocked down.

Acknowledgments

Abbreviations

ECM, extracellular matrix
SEM, standard error of the mean
GP, glycoprotein
qPCR, quantitative PCR
plts, platelets
IL, interleukin
CT, cytoplasmic tail
scr, scrambled
ELISA, Enzyme-Linked ImmunoSorbent Assay
PPP, platelet poor plasma
PRP, platelet rich plasma
ΔΔCt, delta delta cycle threshold equation
HEK, Human Embryonic Kidney cells

References

1. Ginsberg MH, Partridge A, Shattil SJ. Integrin regulation. Curr Opin Cell Biol 2005;17(5):509–516. [PubMed: 16099636]

2. Kieffer N, Phillips DR. Platelet membrane glycoproteins: functions in cellular interactions. Annu Rev Cell Biol 1990;6:329–357. [PubMed: 2275816]

3. Phillips DR, Charo IF, Scarborough RM. GPIIb-IIIa: the responsive integrin. Cell 1991;65(3):359–362. [PubMed: 2018971]

4. Andrews RK, Berndt MC. Platelet physiology and thrombosis. Thromb Res 2004;114(5–6):447–453. [PubMed: 15507277]

5. Naik UP, Patel PM, Parise LV. Identification of a novel calcium-binding protein that interacts with the integrin alphaIIb cytoplasmic domain. J Biol Chem 1997;272(8):4651–4654. [PubMed: 9030514]

6. Gentry HR, Singer AU, Betts L, et al. Structural and biochemical characterization of CIB1 delineates a new family of EF-hand-containing proteins. J Biol Chem 2005;280(9):8407–8415. [PubMed: 15574431]

7. Yamniuk AP, Vogel HJ. Calcium- and magnesium-dependent interactions between calcium- and integrin-binding protein and the integrin alphaIIb cytoplasmic domain. Protein Sci 2005;14(6):1429–1437. [PubMed: 15883187]

8. Wu X, Lieber MR. Interaction between DNA-dependent protein kinase and a novel protein, KIP. Mutat Res 1997;385(1):13–20. [PubMed: 9372844]

9. Kauselmann G, Weiler M, Wulff P, et al. The polo-like protein kinases Fnk and Snk associate with a Ca(2+)- and integrin-binding protein and are regulated dynamically with synaptic plasticity. EMBO J 1999;18(20):5528–5539. [PubMed: 10523297]

10. Leisner TM, Liu M, Jaffer ZM, et al. Essential role of CIB1 in regulating PAK1 activation and cell migration. J Cell Biol 2005;170(3):465–476. [PubMed: 16061695]

11. Stabler SM, Ostrowski LL, Janicki SM, et al. A myristoylated calcium-binding protein that preferentially interacts with the Alzheimer's disease presenilin 2 protein. J Cell Biol 1999;145(6): 1277–1292. [PubMed: 10366599]

12. Naik MU, Naik UP. Calcium-and integrin-binding protein regulates focal adhesion kinase activity during platelet spreading on immobilized fibrinogen. Blood 2003;102(10):3629–3636. [PubMed: 12881299]

13. White C, Yang J, Monteiro MJ, et al. CIB1, a ubiquitously expressed Ca2+-binding protein ligand of the InsP3 receptor Ca2+ release channel. J Biol Chem 2006;281(30):20825–20833. [PubMed: 16723353]

14. Zayed MA, Yuan W, Leisner TM, et al. Calcium- and Integrin-Binding Protein 1 Regulates Endothelial Cells and Ischemia-Induced Pathological and Adaptive Angiogenesis. Circ Res. 2007

15. Yuan W, Leisner TM, McFadden AW, et al. CIB1 is essential for mouse spermatogenesis. Mol Cell Biol 2006;26(22):8507–8514. [PubMed: 16982698]

16. Yuan W, Leisner TM, McFadden AW, et al. CIB1 is an endogenous inhibitor of agonist-induced integrin alphaIIbbeta3 activation. J Cell Biol 2006;172(2):169–175. [PubMed: 16418530]

17. Naik UP, Naik MU. Association of CIB with GPIIb/IIIa during outside-in signaling is required for platelet spreading on fibrinogen. Blood 2003;102(4):1355–1362. [PubMed: 12714504]

18. Shiraga M, Ritchie A, Aidoudi S, et al. Primary megakaryocytes reveal a role for transcription factor NF-E2 in integrin alpha IIb beta 3 signaling. J Cell Biol 1999;147(7):1419–1430. [PubMed: 10613901]

19. Livak KJ, Schmittgen TD. Analysis of relative gene expression data using real-time quantitative PCR and the 2(-Delta Delta C(T)) Method. Methods 2001;25(4):402–408. [PubMed: 11846609]

20. Schefe JH, Lehmann KE, Buschmann IR, et al. Quantitative real-time RT-PCR data analysis: current concepts and the novel "gene expression's CT difference" formula. J Mol Med 2006;84(11):901–910. [PubMed: 16972087]

21. Bairoch A, Apweiler R, Wu CH, et al. The Universal Protein Resource (UniProt). Nucleic Acids Res 2005;33(Database issue):D154–D159. [PubMed: 15608167]

22. Altschul SF, Lipman DJ. Protein database searches for multiple alignments. Proc Natl Acad Sci U S A 1990;87(14):5509–5513. [PubMed: 2196570]

23. Chenna R, Sugawara H, Koike T, et al. Multiple sequence alignment with the Clustal series of programs. Nucleic Acids Res 2003;31(13):3497–3500. [PubMed: 12824352]

24. Subramaniam M, Frenette PS, Saffaripour S, et al. Defects in hemostasis in P-selectin-deficient mice. Blood 1996;87(4):1238–1242. [PubMed: 8608210]

25. Denis CV, Wagner DD. Platelet adhesion receptors and their ligands in mouse models of thrombosis. Arterioscler Thromb Vasc Biol 2007;27(4):728–739. [PubMed: 17272754]

26. Furie B, Furie BC. Thrombus formation in vivo. J Clin Invest 2005;115(12):3355–3362. [PubMed: 16322780]

27. Kurz KD, Main BW, Sandusky GE. Rat model of arterial thrombosis induced by ferric chloride. Thromb Res 1990;60(4):269–280. [PubMed: 2087688]

28. Tsuboi S. Calcium integrin-binding protein activates platelet integrin alpha IIbbeta 3. J Biol Chem 2002;277(3):1919–1923. [PubMed: 11704681]

29. Mayhew MW, Webb DJ, Kovalenko M, et al. Identification of protein networks associated with the PAK1-betaPIX-GIT1-paxillin signaling complex by mass spectrometry. J Proteome Res 2006;5(9): 2417–2423. [PubMed: 16944954]

30. Barry WT, Boudignon-Proudhon C, Shock DD, et al. Molecular basis of CIB binding to the integrin alpha IIb cytoplasmic domain. J Biol Chem 2002;277(32):28877–28883. [PubMed: 12023286]

31. Shock DD, Naik UP, Brittain JE, et al. Calcium-dependent properties of CIB binding to the integrin alphaIIb cytoplasmic domain and translocation to the platelet cytoskeleton. Biochem J 1999;342(Pt 3):729–735. [PubMed: 10477286]

32. Yamniuk AP, Ishida H, Vogel HJ. The interaction between calcium- and integrin-binding protein 1 and the alphaIIb integrin cytoplasmic domain involves a novel C-terminal displacement mechanism. J Biol Chem 2006;281(36):26455–26464. [PubMed: 16825200]

33. Han J, Lim CJ, Watanabe N, et al. Reconstructing and deconstructing agonist-induced activation of integrin alphaIIbbeta3. Curr Biol 2006;16(18):1796–1806. [PubMed: 16979556]

34. Petrich BG, Marchese P, Ruggeri ZM, et al. Talin is required for integrin-mediated platelet function in haemostasis and thrombosis. J Exp Med 2007;204(13):3103–3111. [PubMed: 18086863]

35. Petrich BG, Fogelstrand P, Partridge AW, et al. The antithrombotic potential of selective blockade of talin-dependent integrin alpha IIb beta 3 (platelet GPIIb-IIIa) activation. J Clin Invest 2007;117 (8):2250–2259. [PubMed: 17627302]

36. Leisner TM, Yuan W, Denofrio JC, et al. Tickling the tails: cytoplasmic domain proteins that regulate integrin alphaIIbbeta3 activation. Curr Opin Hematol 2007;14(3):255–261. [PubMed: 17414216]

37. Larkin D, Murphy D, Reilly DF, et al. ICln, a novel integrin alphaIIbbeta3-associated protein, functionally regulates platelet activation. J Biol Chem 2004;279(26):27286–27293. [PubMed: 15075326]

38. Leung-Hagesteijn CY, Milankov K, Michalak M, et al. Cell attachment to extracellular matrix substrates is inhibited upon downregulation of expression of calreticulin, an intracellular integrin alpha-subunit-binding protein. J Cell Sci 1994;107(Pt 3):589–600. [PubMed: 8006073]

39. Liu QY, Corjay M, Feuerstein GZ, et al. Identification and characterization of triosephosphate isomerase that specifically interacts with the integrin alphaIIb cytoplasmic domain. Biochem Pharmacol 2006;72(5):551–557. [PubMed: 16859644]

40. Reilly D, Larkin D, Devocelle M, et al. Calreticulin-independent regulation of the platelet integrin alphaIIbbeta3 by the KVGFFKR alphaIIb-cytoplasmic motif. Platelets 2004;15(1):43–54. [PubMed: 14985176]

41. Vijayan KV, Liu Y, Li TT, et al. Protein phosphatase 1 associates with the integrin alphaIIb subunit and regulates signaling. J Biol Chem 2004;279(32):33039–33042. [PubMed: 15205468]

42. Liu, J.; DeNofrio, J.; Yuan, W.; Wang, Z.; McFadden, AW.; Parise, LV. Genetic Manipulation of Megakaryocytes to Study Platelet Function. In: Gerald, PS., editor. Current Topics in Developmental Biology. Academic Press; 2007. p. 311-335.

43. Vallar L, Melchior C, Plancon S, et al. Divalent cations differentially regulate integrin alphaIIb cytoplasmic tail binding to beta3 and to calcium- and integrin-binding protein. J Biol Chem 1999;274 (24):17257–17266. [PubMed: 10358085]

44. Pearce AC, Senis YA, Billadeau DD, et al. Vav1 and vav3 have critical but redundant roles in mediating platelet activation by collagen. J Biol Chem 2004;279(52):53955–53962. [PubMed: 15456756]

45. Schraw TD, Crawford GL, Ren Q, et al. Platelets from Munc18c heterozygous mice exhibit normal stimulus-induced release. Thromb Haemost 2004;92(4):829–837. [PubMed: 15467915]

46. Pearce AC, McCarty OJ, Calaminus SD, et al. Vav family proteins are required for optimal regulation of PLCgamma2 by integrin alphaIIbbeta3. Biochem J 2007;401(3):753–761. [PubMed: 17054426]

47. Pearce AC, Wilde JI, Doody GM, et al. Vav1, but not Vav2, contributes to platelet aggregation by CRP and thrombin, but neither is required for regulation of phospholipase C. Blood 2002;100(10): 3561–3569. [PubMed: 12411320]
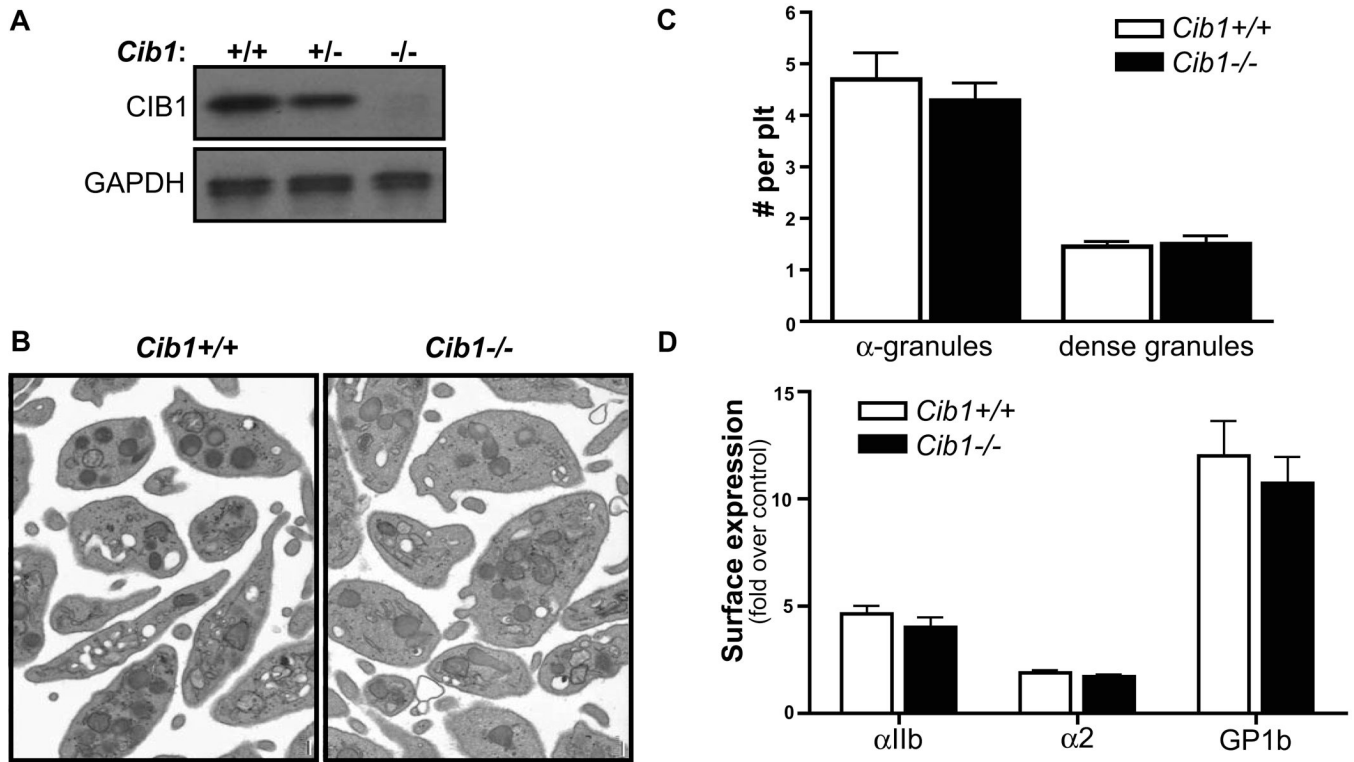
Figure 1. Platelet morphology of *Cib1*^{−/−} mice

A) CIB1 is absent in platelets isolated from the *Cib1*^{−/−} mice. Platelet lysates from *Cib1*^{+/+}, *Cib1*^{+/−} and *Cib1*^{−/−} mice were subjected to Western blotting and CIB1 expression was compared. GAPDH was used as a loading control. B) Resting platelet morphology is normal when examined by electron microscopy. There was no significant difference in size, shape and granule content (C) between *Cib1*^{+/+} and *Cib1*^{−/−} platelets. Scale bar equals 0.2 µM. D) Surface receptor expression on *Cib1*^{−/−} platelets is similar to expression on *Cib1*^{+/+} platelets. To detect surface receptor expression, washed platelets were incubated with FITC-⟨IIb antibody, FITC-⟨2 antibody or FITC-IgG control for 30 min, or FITC-GP1b antibody or FITC-IgG for 15 min at RT. Flow cytometry was used to determine mean fluorescence. Values were normalized and presented as fold over IgG control (antibody/control) (N ≥ 9).
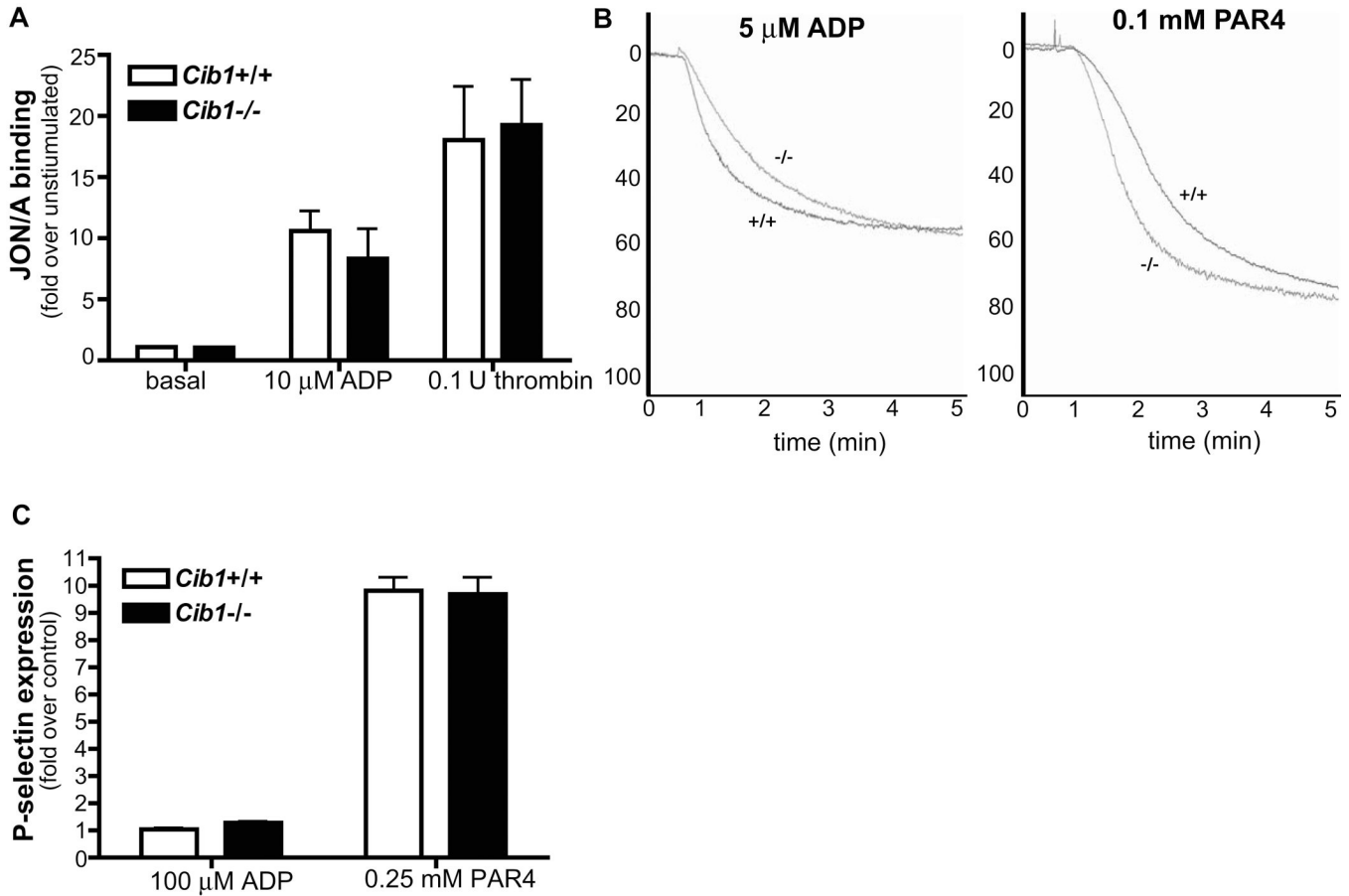
A

B

C

Figure 2. Platelet function is unaffected by the loss of CIB1
A) Integrin ⟨IIb®3 activation is normal when assessed by flow cytometry. Washed platelets were incubated for 15 min with an ⟨IIb®3 active conformation specific antibody (JON/A) or IgG control. Basal expression was defined as JON/A binding over IgG control binding (JON/A antibody/control antibody). Agonist-induced activation was measured by stimulating platelets with either 10 µM ADP or 0.1 U thrombin (per 50 µl reaction) and expressed as the increase in antibody binding in stimulated divided by nonstimulated platelets (N ≥ 4). B) Platelet aggregation is normal in washed $Cib1^{+/+}$ and $Cib1^{-/-}$ platelets. Washed platelets were stimulated by 5 µm ADP (left) or 0.1 mM PAR4 peptide (right) and platelet aggregation traces were recorded for 5 min. Representative traces are shown (N ≥ 2). C) Platelet P-selectin surface expression is not affected by the loss of CIB1 as measured by flow cytometry. P-selectin was expressed on the platelet surface at similar levels after agonist stimulation with 100 mM ADP or 0.25 mM PAR4 peptide (N ≥ 3).
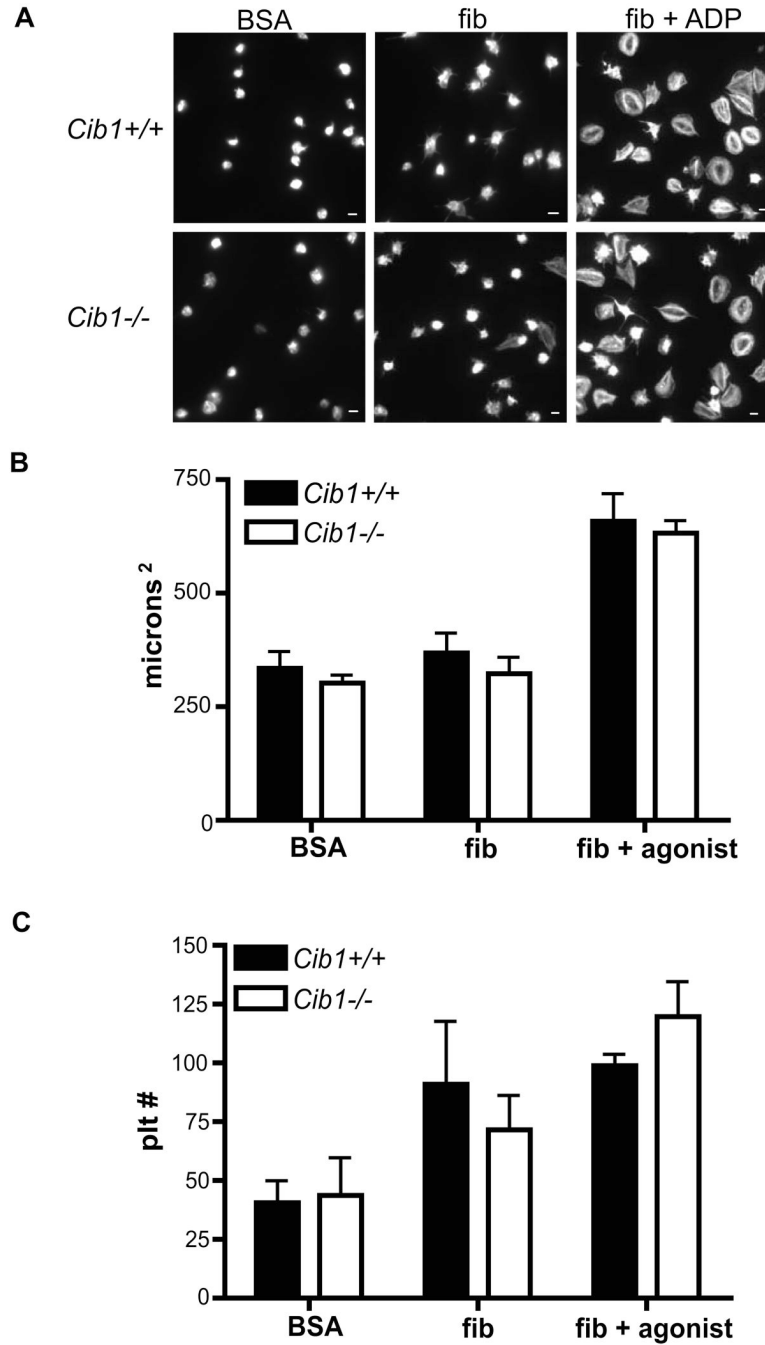
Figure 3. Platelet spreading is normal in the chronic absence of CIB1

A) Platelets from $Cib1^{+/+}$ and $Cib1^{-/-}$ mice adhered and spread similarly on immobilized BSA or fibrinogen (fib). $Cib1^{-/-}$ platelets did not respond differently in the presence or absence 100 µM ADP compared to $Cib1^{+/+}$ platelets. Platelets were allowed to spread for 60 min at 37°C. Scale bar = 1 µm. Platelet size (B) and count (C) were analyzed by ImagePro software and compared between $Cib1^{+/+}$ and $Cib1^{-/-}$. There was no significant difference between the two genotypes (N ≥ 3).
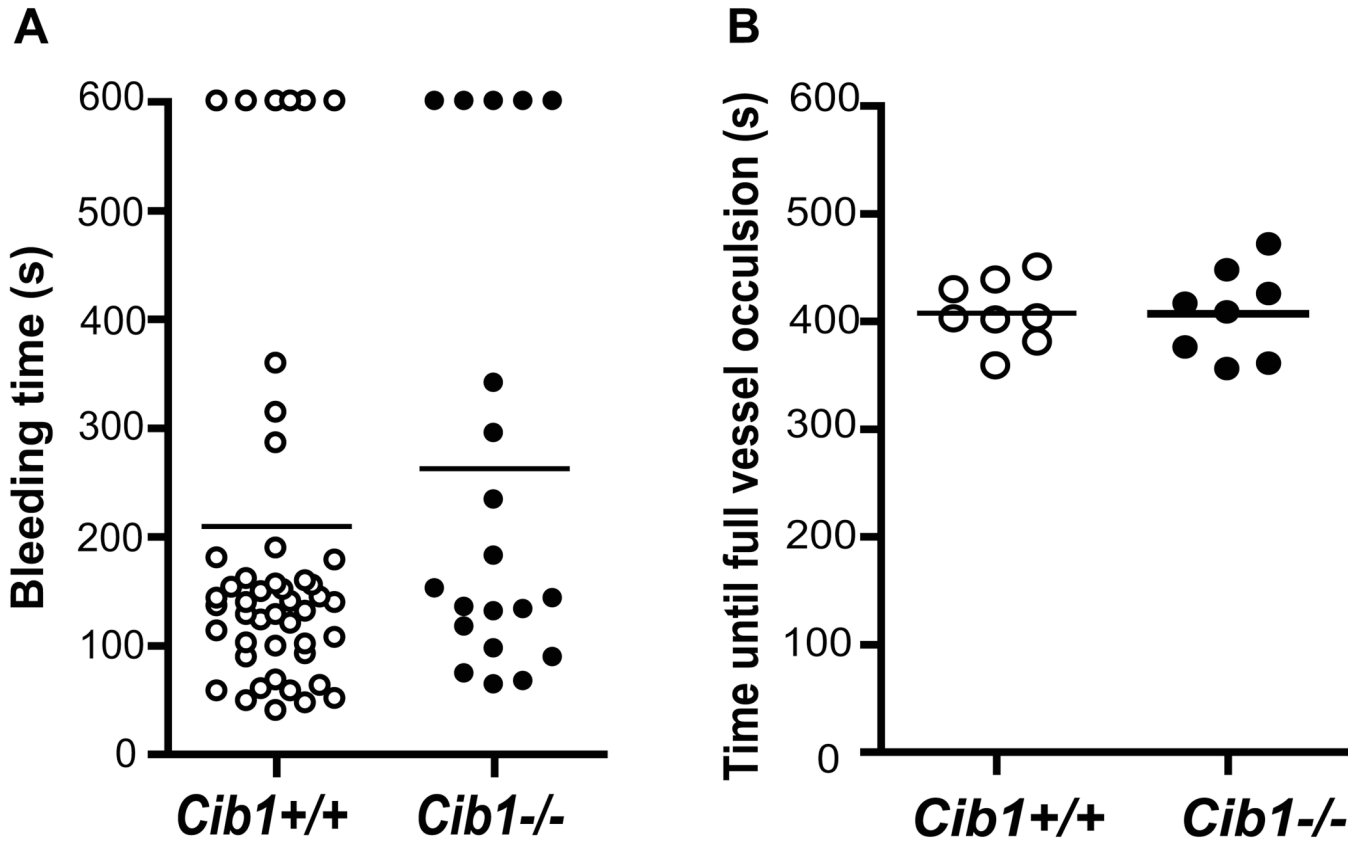
Figure 4. Platelet activation and thrombus formation are normal in *Cib1*^{−/−} mice
A) Bleeding time assay was used to measure thrombus formation and stability in *Cib1*$^{+/+}$ and *Cib1*$^{-/-}$ by cutting the distal 4 mm portion of the tail and recording clotting time. *Cib1*$^{-/-}$ mice had mildly prolonged bleeding time but the difference was not statistically significant from *Cib1*$^{+/+}$ (N ≥ 20 for each genotype). B) Carotid artery thrombosis model was also used to detect differences in thrombus formation and stability. Ferric chloride (20%) saturated paper was placed on the carotid artery to induce injury. Time necessary for full vessel occlusion was recorded and graphed (N = 8 for each genotype).
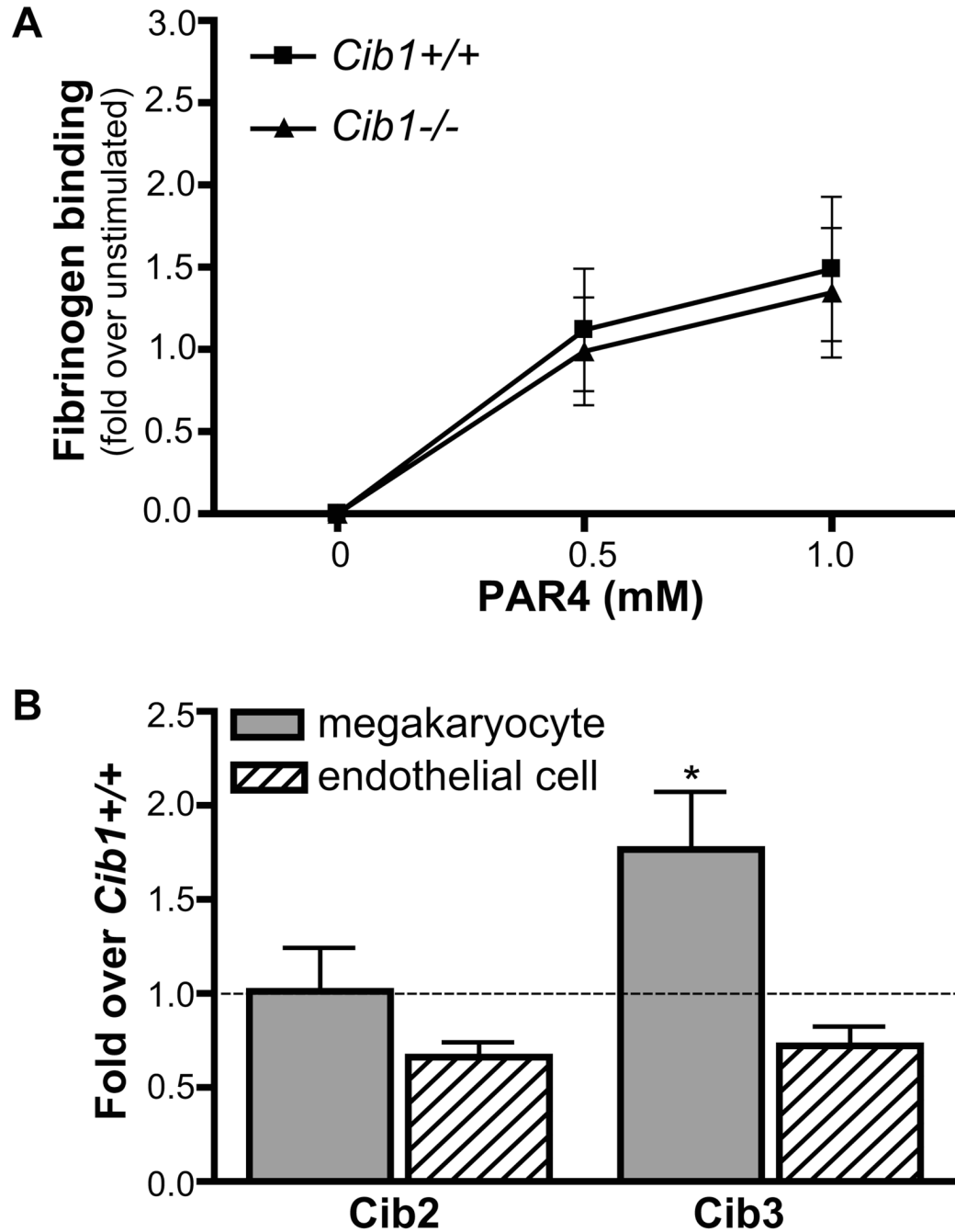
Figure 5. Megakaryocytes from *Cib1*⁻/⁻ mice demonstrate variations in mRNA of CIB family members

A) Activation of integrin αIIbβ3 on cultured bone marrow derived megakaryocytes was similar between *Cib1*+/+ and *Cib1*−/− mice when measured by flow cytometry. Megakaryocytes were stimulated with increasing concentrations of PAR4 peptide (0.5 mM and 1 mM) and binding of Alexa-546 labeled fibrinogen was determined. Mean fluorescent intensities were normalized by dividing the stimulated value by the unstimulated control (N = 3). B) *Cib1*−/− mice have significantly increased CIB3 mRNA in megakaryocytes derived from bone marrow stem cells as measured by quantitative PCR, while CIB2 retains the same level of expression as *Cib1*+/+. *Gapdh* was the housekeeping gene used to normalize cycle threshold (CT) values.

Fold values were defined using the ΔΔCt calculation (Livak et al., 2001; Schefe et al., 2006). Fold value of 1 equates to no change in expression, while values above 1 equal increases in message and values below 1 equal decreases in message expression relative to expression in $Cib1^{+/+}$ cells. Also expression of CIB2 and CIB3 mRNAs are different in $Cib1^{-/-}$ endothelial cells versus megakaryocytes. (N for megakaryocytes $\geq$ 5 and N for endothelial cells = 20).
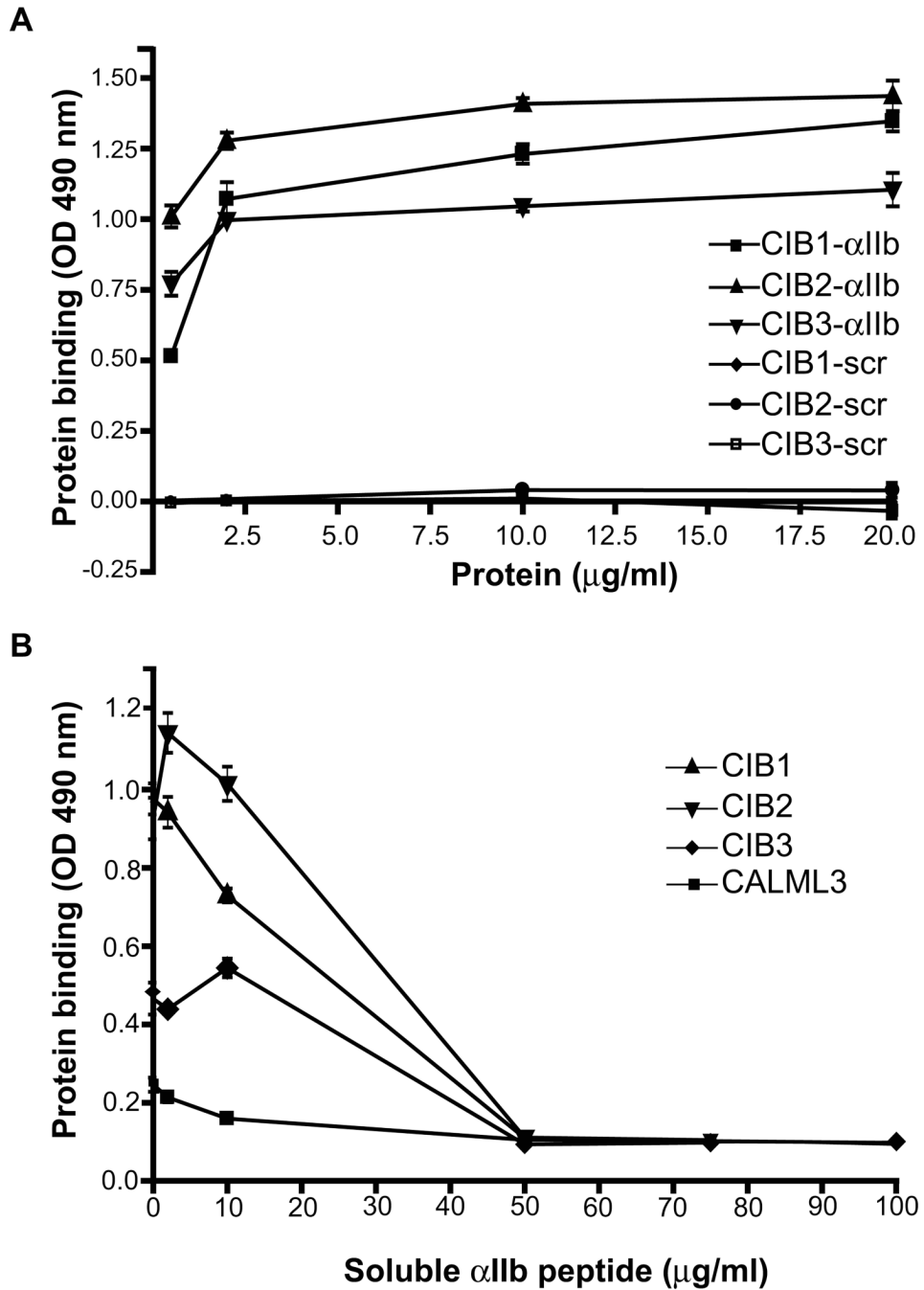
A

B

Figure 6. CIB family members interact with integrin ⟨IIb®3
A) CIB1-3 proteins bind to integrin ⟨IIb peptide as measured by ELISA. Cytoplasmic tail peptides of integrin subunit ⟨IIb (⟨IIb) or a scrambled control (scr) were immobilized and increasing concentrations of recombinant CIB1, -2 or -3 were added to peptide- or BSA-coated wells. Data graphed is a representative experiment of OD 490 (nm) values of peptide-coated wells minus non-specific binding (N = 3). B) Soluble peptide competition ELISAs demonstrate that the CIB1-3 interactions with ⟨IIb peptide are specific. Increasing concentrations of soluble ⟨IIb peptide were incubated with CIB1, -2, -3 or control protein, calmodulin-like 3, for 30 min.

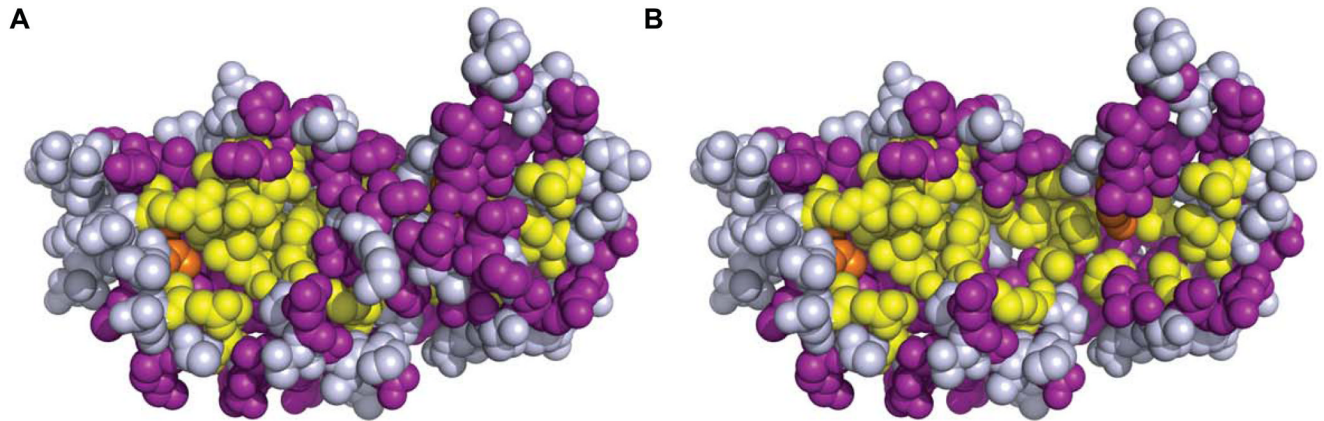Samples were added to immobilized ⟨IIb peptide or BSA coated wells. Data is presented as in (B) (N = 3).

Figure 7. Computer modeling of CIB family proteins reveals a highly conserved hydrophobic binding pocket
A) Homology map of CIB proteins based on the ancestral CIB found in *C. elegans*. Grey represents non-conserved residues, purple represents conserved residues, yellow represents conserved residues in the hydrophobic binding pocket and orange represents non-conserved residues in the hydrophobic binding pocket. B) Model of CIB after displacement of the C-terminal tail. Molecular surfaces are represented as in (A).